Iraqi Journal of Physics, 2020 *Vol.18, No.47, PP. 84-90*

DOI: 10.30723/ijp.18.47.84-90

Coupled Channels Calculations of Fusion Reactions for ^{46}Ti+^{64}Ni, ^{40}Ca+^{194}Pt and ^{40}Ar+^{148}Sm Systems

Hayder J. Musa[1], Fouad A. Majeed[2], Ali T. Mohi[1]

[1]Department of Physics, College of Education, Al- Mustansiriyah University

[2]Department of Physics, College of Education for Pure Sciences, University of Babylon

Corresponding author: hayder.jasim@uokerbala.edu.iq

Abstract

In this work, the fusion cross section σ_{fus}, fusion barrier distribution D_{fus} and the probability of fusion P_{fus} have been investigated by coupled channel method for the systems ^{46}Ti+^{64}Ni, ^{40}Ca+^{194}Pt and ^{40}Ar+^{148}Sm with semi-classical and quantum mechanical approach. By comparing the results of these calculations with the available experimental data, which showed that the quantum mechanical calculations below the fusion barrier agree well with the experimental data of the above systems, while at energies above this barrier, the quantum and semi-classical calculations can reproduce the experimental data.

Key words

Semi-classical treatment, quantum treatment, medium systems, coupled channels.

Article info.

Received: Sep. 2020
Accepted: Nov. 2020
Published: Dec. 2020

حسابات اقتران القنوات لتفاعلات الاندماج للأنظمة ^{46}Ti+^{64}Ni، ^{40}Ca+^{194}Pt و ^{40}Ar+^{148}Sm

حيدر جاسم موسى[1]، فؤاد عطية مجيد[2]، علي طاهر محي[1]

[1]قسم الفيزياء، كلية التربية، الجامعة المستنصرية

[2]قسم الفيزياء، كلية التربية للعلوم الصرفة، جامعة بابل

الخلاصة

في العمل الحالي، تم ايجاد مساحة مقطع الاندماج σ_{fus}، توزيع حاجز الاندماج D_{fus} اضافة الى احتمالية الاندماج P_{fus} بطريقة اقتران القنوات للأنظمة ^{46}Ti+^{64}Ni، ^{40}Ca+^{194}Pt و ^{40}Ar+^{148}Sm وفق التقريب الشبه كلاسيكي والكمي. من خلال مقارنة نتائج هذه الحسابات مع البيانات التجريبية المتوفرة والتي اظهرت ان نتائج الحسابات الكمية اسفل حاجز الاندماج تتوافق بصورة جيدة مع البيانات التجريبية للأنظمة اعلاه بينما عند طاقات اعلى من طاقة الحاجز فان الحسابات الكمية والشبه الكلاسيكية يمكنها اعادة انتاج البيانات التجريبية.

Introduction

In the processes of the colliding nuclei, when the two separate nuclei are overcoming the Coulomb barrier, and fuse together to produce a compound nucleus, this process is known as fusion reactions. The Coulomb barrier is a resultant of a repulsion Coulomb and attractive nuclear forces. At energies below this barrier (classically forbidden region), fusion can take place by tunneling phenomenon. The tunneling probability or transmission coefficient can be evaluated by Wentzel–Kramers–Brillouin (WKB) method [1]. For light nuclei, the probability of fusion

can be described by this barrier with the radial motion between nuclei which represent the only degree of freedom. But medium and heavy nuclei, have internal degrees of freedom and coupling between these and transitional motion can enhances the fusion cross section below the barrier [2-5]. This coupling can by represented by taking into account the rotational deformations, vibrational modes or nucleons transfer processes [1, 6]. The best method to investigate this coupling is the solution of coupled channel equations which are performed with semi-classical approach of Alder and Winther (AW) method for Continuum Discretized Coupled Channel (CDCC) where generalized from Coulomb excitations to nuclear reactions [7].

In the present work, the CDCC method was adopted to evaluate the fusion cross section, fusion barrier distribution and the probability of fusion for the medium systems ^{46}Ti+^{64}Ni, ^{40}Ca+^{194}Pt and ^{40}Ar+^{148}Sm, with SCF code, recently adopted by [8]. The results of this approach were compared with full quantum mechanical calculations which were performed by CCFULL code and recently been adopted by [5], in addition to the available experimental data for these systems.

Theoretical framework

Evaluate the fusion cross section σ_{fus} in the semi-classical coupled channels model, was done by solving AD equations for CDCC method. This procedure was performed by researchers [9-12]. The σ_{fus} for all channels (α) is given by:

$$\boldsymbol{\sigma_{fus} = \frac{\pi}{k^2}\sum_{\alpha}(2\ell + 1)\, P_{\ell}(\alpha)} \qquad \textbf{(1)}$$

where k is the wave number, ℓ represents the orbital quantum number and the probability of fusion is $P_{\ell}(\alpha)$, which is expressed by [10, 12, 13]

$$\boldsymbol{P_{\ell}(\alpha) = \frac{4k}{E}\int |u_{\ell}(k,r)|^2 w_{\alpha}(r)\, dr} \qquad \textbf{(2)}$$

where $u_{\ell}(k,r)$ is the radial wave equation for the ℓ th partial wave in channel α, E represents the center of mass energy and $w_{\alpha}(r)$ is the imaginary part of the optical potential associated to fusion in this channel.

In the quantum mechanical calculation, the σ_{fus} for no- Coriolis approximation is given by [1]:

$$\boldsymbol{\sigma_{fus} = \frac{\pi}{k^2}\sum_{\alpha}(2J + 1)\, P_{J}(E)} \qquad \textbf{(3)}$$

where J is the total angular momentum.

In the coupling, the barrier can be thought as a set of subbarriers or barrier distribution, and the fusion occurs by these subbarriers. The fusion barrier distribution $D_{fus}$is an important tool to investigate the mechanism of fusion and nuclear structure of colliding nuclei [1, 3, 14]. Rowley et al. found the expression to evaluate this function by the experimental data of σ_{fus} [15].

$$\boldsymbol{D_{fus} = \frac{d^2(E\sigma)}{dE^2}} \qquad (\mathbf{4})$$

which was found theoretically from σ_{fus} by three point difference method [3,16]

$$\boldsymbol{D_{fus} = 2\left[\frac{(E\sigma)_3 - (E\sigma)_2}{E_3 - E_2} - \frac{(E\sigma)_2 - (E\sigma)_1}{E_2 - E_1}\right]\left(\frac{1}{E_3 - E_1}\right)} \qquad (\mathbf{5})$$

At energy (E_1+2E_2+E_3)/4 and for equal spacing between the values of energy (ΔE), the above equation can be written as

$$\boldsymbol{D_{fus} = \frac{(E\sigma)_3 - 2(E\sigma)_2 + (E\sigma)_1}{(\Delta E)^2}} \qquad (\mathbf{6})$$

The second derivative statistical error is give as [16]

$$\delta_c \cong \frac{E}{\Delta E^2}\sqrt{\rho_1^2 + 4\rho_2^2 + \rho_3^2} \qquad (7)$$

where ρ is the absolute cross section uncertainties.

Results and discussion

The semi-classical coupled channels calculations for the systems ^{46}Ti+^{64}Ni, ^{40}Ca+^{194}Pt and ^{40}Ar+^{148}Sm have been performed by SCF code to evaluate fusion cross section, fusion barrier distribution and the probability of fusion. These results were compared with the available experimental data and full quantum mechanical calculations which were carried out by CCFULL code with two modes of excitation both in projectile and target nuclei.

The real parameters of nuclear potential, Wood-Saxon potential, for the above systems which were obtained by fitting the experimental data of fusion cross sections are listed in Table 1, where $V_\circ$ is the potential depth, $r_\circ$ is the radius constant and diffuseness $a_\circ$.

Table 1: Parameters of Wood-Saxon potential.

System	$V_\circ$ (MeV)	$r_\circ$ (fm)	$a_\circ$ (fm)
^{46}Ti+^{64}Ni	93	1.17	0.71
^{40}Ca+^{194}Pt	160	1.14	0.73
^{40}Ar+^{148}Sm	240	1.14	0.78

1. The ^{46}Ti+^{64}Ni system

In the quantum mechanical calculations, the vibrational coupling with single phonon for Ti and Ni was taken into account. The deformation parameters β corresponding to multipolarity λ are listed in Table 2. Theσ_{fus}, D_{fus} and P_{fu} results are shown in Fig.1 panels a, b and c, respectively. The measured data (green circles) were taken for this system from [17]. Below the Coulomb barrier V_b, as indicated by the (magenta arrow on the $E_{c.m.}$ axis) the calculations of quantum mechanics (the red curve) forσ_{fus}, performed by (CCFULL) are in better agreement with the measured data, as shown in Fig.1 panel (a), while the semi-classical results (black curve), which were accomplished by SCF code are shortfall the data. Above V_b, despite the results of CCFLL code are closest to the data, but the results of SCF code for σ_{fus} are close as well.

For D_{fus} calculations, Fig.1 panel (b), the results of CCFULL show two peaks of barriers around V_b while only one peak appears in SCF results. These peaks in quantum calculations gives an enhanced sub-barrier fusion as shown in panel (a), especially below V_b. Fig.1.c illustrates the results of probability of fusion, below V_b, quantum mechanical results are closer to the data than the results of SCF code, for the same reason above. Above V_b, the results of calculations are matching the experimental data.

This enhancement in quantum calculations below the barrier of fusion is due to the coupling to the vibrational excitations, which included low lying states 2^+ and 3^- for participant nuclei, leading to contribution of these channels in the reaction.

Table: 2 The deformation parameters [18, 19].

Isotope	Λ	β
^{46}Ti	3^- 2^+	0.142 0.3175
^{64}Ni	3^- 2^+	0.201 0.1686
^{40}Ca	3^- 2^+	0.411 0.1196
^{194}Pt	2^+	0.1421
^{40}Ar	3^- 2^+	0.341 0.2602
^{148}Sm	3^- 2^+	0.158 0.1416

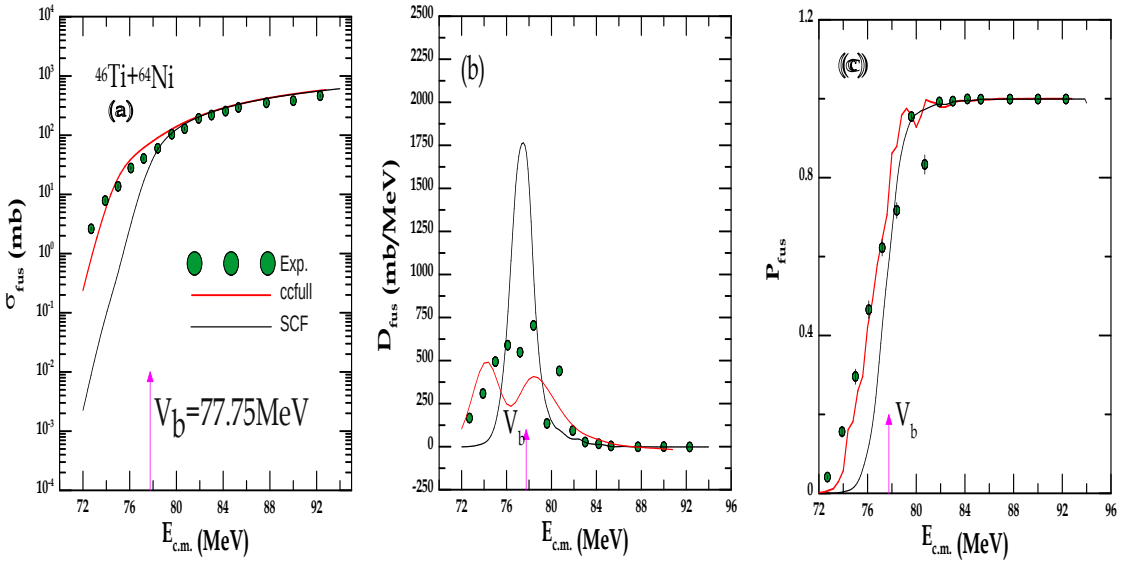

Fig. 1: (a) The cross section of fusion, (b) the distribution of fusion barrier and (c) the probability of fusion for the system ^{46}Ti+^{64}Ni (red curve represent the quantum mechanical calculations, black curve represents the semi-classical calculations, green circles are experimental data [17], the barrier position indicated by magenta arrow on the $E_{c.m}$ axis).

2. The ^{40}Ca+^{194}Pt system

Fig. 2 (a, b and c) represent theσ_{fus}, D_{fus} and P_{fus} for this system. The experimental data were taken from [20]. The quantum mechanical calculations were performed with two modes of vibrational excitation of projectile and single mode of vibrational excitation of target with two phonons for both projectile and target nuclei. The deformation parameters for this system are listed in Table 2. As shown in Fig.2(a), the results of CCFULL code for σ_f (red curve) with low lying states 2^+ and 3^- for Ca nucleus and 2^+ state for Pt nucleus with two phonons for both nuclei at energies below V_b are closer to experimental data than the results of SCF code, as shown in Fig.2(a). While above V_b, the two curves are coincide with the experimental data. As shown in the Fig. 2(a), although the results of CCFULL code are better than that of the SCF code below the barrier, but it is still less than the data at these energies. This reduction in calculations below the fusion barrier indicates the presence of other channels of interaction below this barrier. When adding the two-neutron

pickup channel to the excitation due to vibration channel, a significant enhancement in the results below the barrier were noticed, as shown in the blue curve in this figure. Ground state energy of neutron transfer channel for this reaction Q_{gg} is equal to 5.23MeV and the configuration factor was arbitrarily chosen to be (0.9) to obtain this enhancement.

The results of fusion barrier distribution Fig. 2(b), shows a spectrum of barriers around V_b for the quantum calculations, (red curve), while there was only a single barrier for the semi-classical calculations. These results explain the improvement in σ_{fus} for the quantum calculations. The results of CCFULL code was obtained with vibrational excitations which show more than one barrier. These barriers correspond to different channels of interaction which did not appear in the semi-classical calculations as these calculations do not include the interaction channels resulting from the deformations of the interacting nuclei.

The probability of fusion, Fig.2(c), shows that the results of the quantum calculation well match the experimental data below V_b, while at energies above V_b the two curves are well match the experimental data.

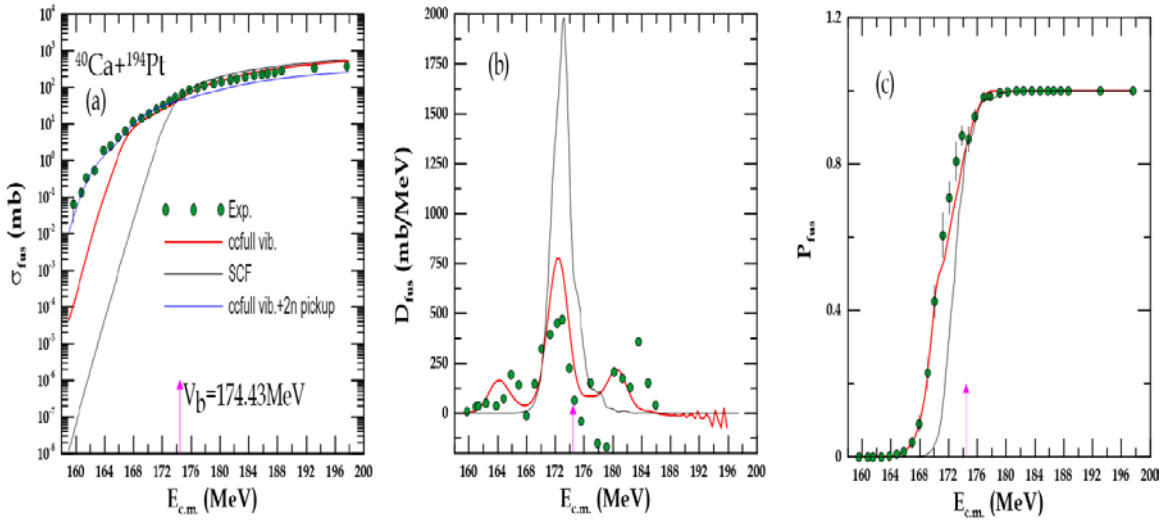

Fig.2: (a) The cross section of fusion, (b) the distribution of fusion barrier and (c) the probability of fusion for the system $^{40}Ca+^{194}Pt$ (red and blue curves represent the quantum mechanical calculations, black curve represents the semi-classical calculations, green circles are experimental data [20], the barrier position indicated by magenta arrow on the $E_{c.m}$ axis).

3. The $^{40}Ar+^{148}Sm$ system

The results of σ_{fus}, D_{fus} and P_{fus} calculations for this system shows in Fig. 3(a, b and c). Two modes of vibrational coupling for colliding nuclei with single phonon is adopted in this system. The parameters of deformation are listed in Table 2. The results of σ_{fus}, Fig. 3(a) shows a better agreement for both CCFULL and SCF codes with the experimental data which were taken from [21]. In quantum calculations, the coupling of low-lying states of 2^+ and 3^- levels were adopted which corresponding to quadrupole and octupole vibration in nuclei.

The D_{fus} of this system, Fig. 3(b) shows that the red curve of CCFULL code has god fit with the experimental data than the black curve of SCF code. Fig.3(c), represents the probability of fusion, the two curves are coincide and well represent the data.

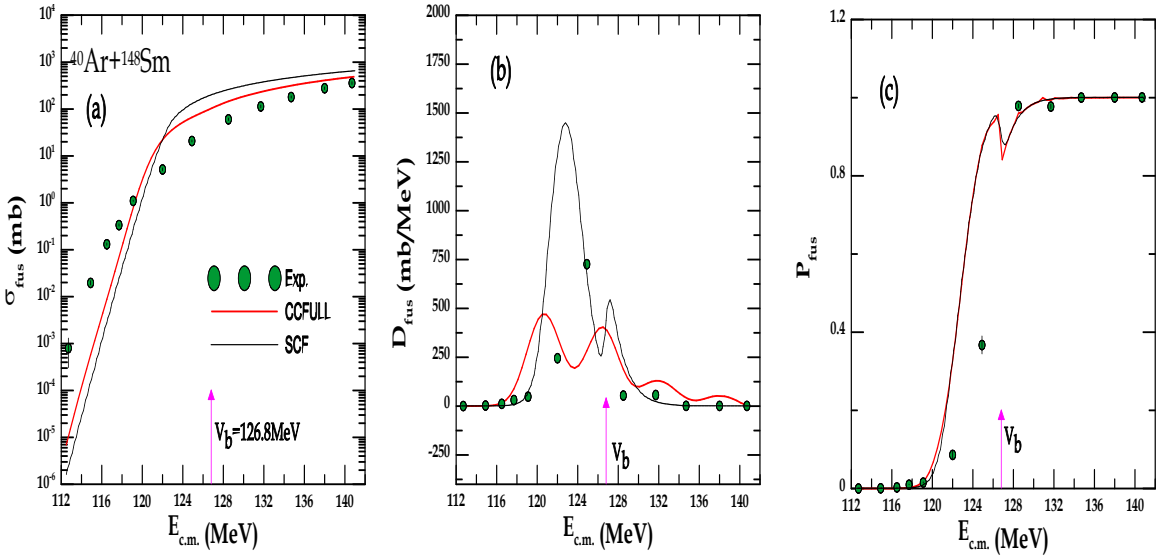

Fig.3: (a) The cross section of fusion, (b) the distribution of fusion barrier and (c) the probability of fusion for the system $^{40}Ar+^{148}Sm$ (red curve represent the quantum mechanical calculations, s black curve represents the semi-classical calculations, green circles are experimental data [21], the barrier position indicated by magenta arrow on the $E_{c.m}$ axis).

Conclusions

In this study, the results of the full quantum mechanics forσ_{fus}, D_{fus} andP_{fus}, are better than the semi-classical results especially below the Coulomb barrier of the studied systems. Whereas, the effect of introducing the deformation parameters for the colliding nuclei, as well as the coupling to vibrational states and neutrons transfer processes, in the quantum calculations led to a remarkable enhancement in the results of these calculations below the fusion barrier. While above this barrier, the semi-classical and the quantum calculations reproduced the experimental data for these systems.

Acknowledgment

The authors are very grateful to Dr. Adil J. Nagim for his kind help in performing the ccfull calculations and the author F. A. Majeed is very grateful to TWAS-CNPq for one-year post-doc and UFRJ warm hospitality.

References

[1] K. Hagino and N. Takigawa, Prog. Theor. Phys.,128, 6 (2012) 1061-1106.
[2] C. H. Dasso, S. Landowne, A. Winther, Nucl. Phys. A, 405, 2 (1983) 381-396.
[3] M. Dasgupta, D. J. Hinde, N. Rowley, A. M. Stefanini, Annu. Rev. Nucl. Part. Sci., 48, 1 (1998) 401-461.
[4] A. B. Balantekin and N. Takigawa, “Quantum tunneling in nuclear fusion,” Rev. Mod. Phys., 70, 1 (1998) 77-100.
[5] R. Fereidonnejad, H. Sadeghi, M. Ghambari, Astrophys. Space Sci., 363, 3 (2018) 50.
[6] P. Fröbrich and R. Lipperheide, "Theory of nuclear reactions", Clarendon Press, 1996.
[7] H. D. Marta, L. F. Canto, R. Donangelo, P. Lotti, Phys. Rev. C, 66, 2 (2002) 246051-246055.
[8] H. J. Musa, F. A. Majeed, A. T. Mohi, IOP Conference Series: Materials Science

and Engineering, 871, 1 (2020) 12063-1_12063-7.
[9] F. M. Hussain, F. A. Majeed, Y. A. Abdul-Hussien, IOP Conference Series: Materials Science and Engineering, 571, 1 (2019) 12113-1_12113-7.
[10] M. S. Hussein, L. F. Canto, R. Donangelo, "A New Era of Nuclear Structure Physics, World Scientific, (2004) 124-129.
[11] F. A. Majeed, Int. J. Nucl. Energy Sci. Technol., 11, 3 (2017) 218-228.
[12] L. F. Canto, P. R. S. Gomes, R. Donangelo, M. S. Hussein, Phys. Rep., 424, 1–2 (2006) 1-111.
[13] L. F. Canto, R. Donangelo, H. D. Marta, Phys. Rev. C, 73, 3 (2006) 34608.
[14] S. V. S. Sastry and S. Santra, Pramana, 54, 6 (2000) 813-826.
[15] N. Rowley, G. R. Satchler, P. H. Stelson, Phys. Lett. B, 254, 1–2 (1991) 25-29.
[16] A. J. Najim, F. A. Majeed, K. H. Al-Attiyah, IOP Conference Series: Materials Science and Engineering, 571, 1 (2019) 12124-1_12124-5.
[17] N. Prasad, A.M. Vinodkumar, A.K. Sinha, K.M. Varier, D.L. Sastry, N. Madhavan, P. Sugathan, D.O. Kataria, J.J. Das, Nucl. Phys. A, 603, 2 (1996) 176-202.
[18] T. Kibedi and R. H. Spear, At. Data Nucl. Data Tables, 80, 1 (2002) 35-82.
[19] B. Pritychenko, M. Birch, B. Singh, M. Horoi, At. Data Nucl. Data Tables, 107 (2016) 1-139.
[20] J. D. Bierman, P. Chan, J. F. Liang, M. P. Kelly, A. A. Sonzogni, R. Vandenbosch, Phys. Rev. C, 54, 6 (1996) 3068-3075.
[21] W. Reisdorf, F.P. Hesberger, K.D. Hildenbrand, S. Hofmann, G. Münzenberg, K.H. Schmidt, J.H.R. Schneider, W.F.W. Schneider, K. Sümmerer, G. Wirth, J.V. Kratz, K. Schlitt, Nucl. Phys. A, 438, 1 (1985) 212-252.